Ignition of Premixed Air/Fuel Mixtures by Microwave Streamer Discharge

P. Denissenko[a,*], M.P. Bulat[b,e], I.I. Esakov[c], L.P. Grachev[c], K.N. Volkov[d], I.A. Volobuev[e], V. Upyrev[e], P.V. Bulat[b,e]

[a]*School of Engineering, University of Warwick, CV4 7AL, Coventry, UK*
[b]*Baltic State Technical University Voenmeh, 190005, St Petersburg, Russia*
[c]*Moscow Radiotechnical Institute of RAS, 117519, Moscow, Russia*
[d]*Kingston University, SW15 3DW, London, UK*
[e]*ITMO University, 197101, St Petersburg, Russia*

Abstract

A variety of methods exists for fast and efficient combustion of air-fuel mixtures. In this study, a microwave subcritical streamer discharge is used to ignite propane-air mixtures at atmospheric pressure. The streamer is initiated at the inner surface of a dielectric tube with the help of a passive half-wave vibrator. By creating a network of ignition lines, the streamer discharge forms the network of burning channels with large total surface area. This leads to the apparent speed of combustion propagation along the cylinder in excess of 100 m/s, which is more than 200 times the laminar flame propagation speed. The axial propagation of the combustion front in a cylindrical tube filled with the air/propane mixture is investigated by high speed video recording in visible light. A simple model is presented to explain observed results.

Keywords: Microwave, Streamer discharge, Air-Fuel Mixture, Ignition, Plasma-Assisted Combustion,

1. Introduction

Increasing the burning rate of fuel leads to a higher specific engine power, reduction of emissions of nitrogen oxides, and the possibility of burning lean

*Corresponding author
Email address: p.denissenko@gmail.com (P. Denissenko)

or diluted air-fuel mixtures [1]. Optimisation of the ignition system has always posed challenges in commercial applications. Conventional spark plug systems have several limitations including inability to ignite lean mixtures, only providing a localized ignition, and being prone to cathode erosion. Many experimental, theoretical and numerical studies have been performed in the past years with a variety of ignition systems such as electric discharge, microwave discharge, and laser radiation [2, 3, 4] tested to achieve simultaneous ignition at multiple ignition points throughout the combustion chamber. Plasma-assisted combustion is a promising technique to improve engine efficiency, reduce emissions, and enhance fuel reforming [1, 5, 6] with the use of cold and non-thermal plasmas appearing in microwave discharges becoming a major topic of interest [7, 8].

The idea of using plasma methods of fuel ignition is based on non-equilibrium generation of chemically active molecules, accelerating the combustion process [9]. Mechanisms for the acceleration of combustion under the action of a non-equilibrium plasma are actively discussed including the generation of atomic oxygen and other chemical radicals [10], development of molecules of singlet delta-oxygen [11, 12], and chain ion-molecular reactions with intermediate radicals [13]. The use of a non-equilibrium electric discharge is experimentally demonstrated in [14, 15, 16]. Results of experimental and numerical analysis of plasma-assisted combustion at a normal and high pressures and temperatures are presented in [17].

Microwave plasma has shown potential to improve ignition characteristics [18, 19]. Microwave plasma can be generated at pressures from 10^{-5} torr up to atmospheric pressure in pulsed and continuous regimes. Meanwhile, a powerful microwave generator is required at the atmospheric pressure when the breakdown takes place at the energy density larger than 10^6 W/cm^2. A volume microwave discharge is used in the ignition systems [20] and combustion stabilizers [21]. The study [22] investigates experimentally the minimum energy necessary to ignite a premixed air-methane mixture. A thermal spark promotes neutral heating by maintaining the electrical current over a long period which is less efficient in the end [23].

Among various types of discharges studied, the subcritical microwave streamer discharge has recently demonstrated promising characteristics for ignition at low initial temperatures [24]. The streamer discharge represents a random network of plasma channels (filaments) with the characteristic diameter of a fraction of a millimetre, and a characteristic distance between the channels of a fraction of the radiation wavelength [25, 26, 27]. Streamers are non-thermal filamentary plasmas developing in insulating medium under the influence of strong external electric fields [28]. A notable property of a developed streamer discharge is that it absorbs almost all the electromagnetic energy incident on it. An important feature of streamer discharges is that the streamers of which they are comprised, like streamers in constant electric field, grow to regions where the magnitude of the electric field is substantially below the critical breakdown value. Therefore, once initiated, a subcritical streamer discharge spreads in a considerable volume, requiring the power much smaller than that to initiate a critical discharge. The energy deposition in air-hydrogen mixture necessary for ignition by streamer discharges is examined in [29].

In this study, possibilities of using the microwave radiation to initiate combustion of premixed air-fuel mixtures are investigated experimentally. The streamer discharge initiated at the tips of a half-wave wire spreads along a dielectric surface in electrical field of a strength several times smaller than the air breakdown value. The flow induced by expansion of combustion products drives the apparent flame propagation speed hundreds times higher than its value of around 0.4 m/s in otherwise still gas mixture [30].

2. Experimental setup

The test rig shown in the Fig. 1 consists of a microwave source, focusing elements, and the tube filled with the air-fuel mixture. The main component of the microwave source is a pulsed magnetron generator. Its power supply is provided by a modulator based on a partial discharge of a storage capacitor. The maximum pulsed power of the magnetron is about 10^7 W. The modulator

is used to generate a rectangular 40 μs pulse of 3.4 GHz (8.9 cm) microwave.

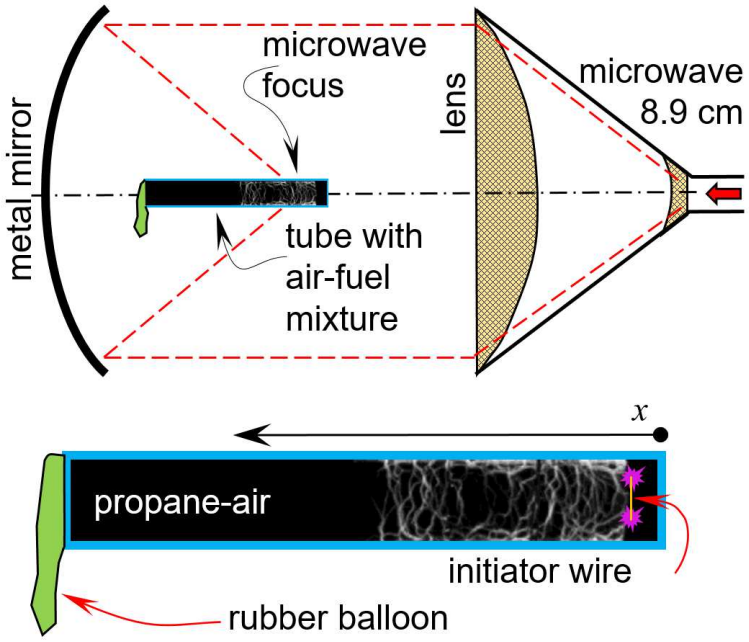

Figure 1: Experimental setup consisting of a system of lenses, a focussing mirror, and an acrylic tube filled with air-fuel mixture. The red dashed line indicates the microwave beam.

The microwave radiation from magnetron is transported through the waveguide, which includes a circulator, an attenuator, a polarizer and a system of dielectric lenses. The waveguide has a rectangular cross-section of 72 mm^2 before the polarizer with a transition to a round cross section (76 mm diameter) at the polarizer. The lens system consists of the lens on the target diffuser of the waveguide and the polystyrene lens forming a quasi-optical beam. It provides input of the microwave radiation into the chamber in transverse electromagnetic mode with a flat phase front and Gaussian intensity distribution. A metal mirror of 685 mm diameter and 450 mm radius of curvature is installed at 1 m from the lens. The mirror focuses the microwave radiation at the axis of the system forming a quasi-optical microwave beam with the strength of electric field at the level of 2 kV/cm. The streamer discharge originates at the tips of the initiator which is a half-wavelength metal wire.

Combustion of the air-propane mixture was selected for experiments as one of the most classical and the most studied processes.

An acrylic tube filled with fuel-air mixture is placed in the focal region of the quasi-optical beam. One end of the tube is blocked, another is equipped with a balloon containing the air-fuel mixture within the tube while keeping the pressure atmospheric. The tube length is 350 mm and its internal diameter is 30 mm. Composition of the air-propane mixture is controlled by varying gas partial pressures when filling the tube. The measurements have been performed with mixtures of stoichiometric ratio of 1, 0.87, and 1.33.

The discharge initiator, a half-wavelength wire, is placed at 27 mm from the closed end of the tube. The streamer initiates at the tips of the wire where the electric field is above the critical value. Once appeared at the initiator, the net of streamers grows towards the metal mirror i.e. towards the direction from which the focussed microwave beam arrives. As seen in Fig.2, streamer propagation in the other direction is suppressed because conductive plasma filaments shade that area from the higher intensity microwave radiation focussed by the mirror.

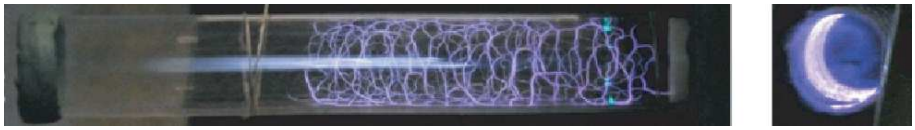

Figure 2: Streamer discharge initiated at the inner surface of the tube: side view and the front view, a long exposure photo. The blue-green spots indicate streamer initiation points at the tips of the half-wave wire.

The evolution of combustion-filled volume has been recorded in visible light using a monochrome high-speed camera Phantom v.2511 at frame rates of up to 10,000 frames/s. The speed of the combustion front propagation has been measured from spatio-temporal images constructed from the acquired videos.

3. Experimental results

Due to the short, 40μs, duration of the microwave pulse, combustion of the gas mixture may be assumed to start simultaneously along the entire length

of discharge filaments. Then, two processes influence the combustion. The burning filaments thicken due to the flame propagation and also due to the expansion of combustion products. In this way, a region spanned by combustion with somewhat turbulent flow forms. This region acts as a "piston" of hot gas pushing the fresh unburned mixture towards the open end of the tube. A typical sequence of images is shown in Fig. 3. The length of the streamer discharge was measured using the first frame of image sequences.

To assess the combustion front propagation, spatio-temporal images have been produced such as shown in Fig. 4. In spatio-temporal images, each horizontal row of pixels represents the brightness along the tube axis averaged across the tube. The bright area occupied by combustion products is clearly seen. The slope of the line bounding the combustion area from above corresponds to the inverse flame propagation speed. Observe the fast, up to 80 m/s, growth of the combustion region towards the open (left) end of the tube, and a slow, at the level of 1 m/s, propagation of the flame towards the closed (right) end of the tube. The oscillations of the right boundary caused by compression waves arising in the tube with a closed end: indeed, the oscillation period at the level of 1-2 ms is consistent with the frequency of a sound wave of a quarter-wavelength equal to the tube length of 35 cm. The magnitude of oscillations suggest pressure variations in the tube at the level of 20%.

The measured rate of expansion of the area span by combustion at the tube exit is shown in Fig. 5 for stoichiometric ratios of 1, 0.87, and 1.33. The error bars reflect the range of streamer lengths and expansion rates appearing visually feasible when processing spatiotemporal diagrams similar to that in Fig. 4.

4. Results and Discussion

The anomalously high visible flame propagation rate can be caused by two factors. The first is the large area of the actual flame front formed at the surface of streamer channels. The elevated temperature and pressure in the vicinity of the streamer may also cause the autoignition of the fuel mixture which would

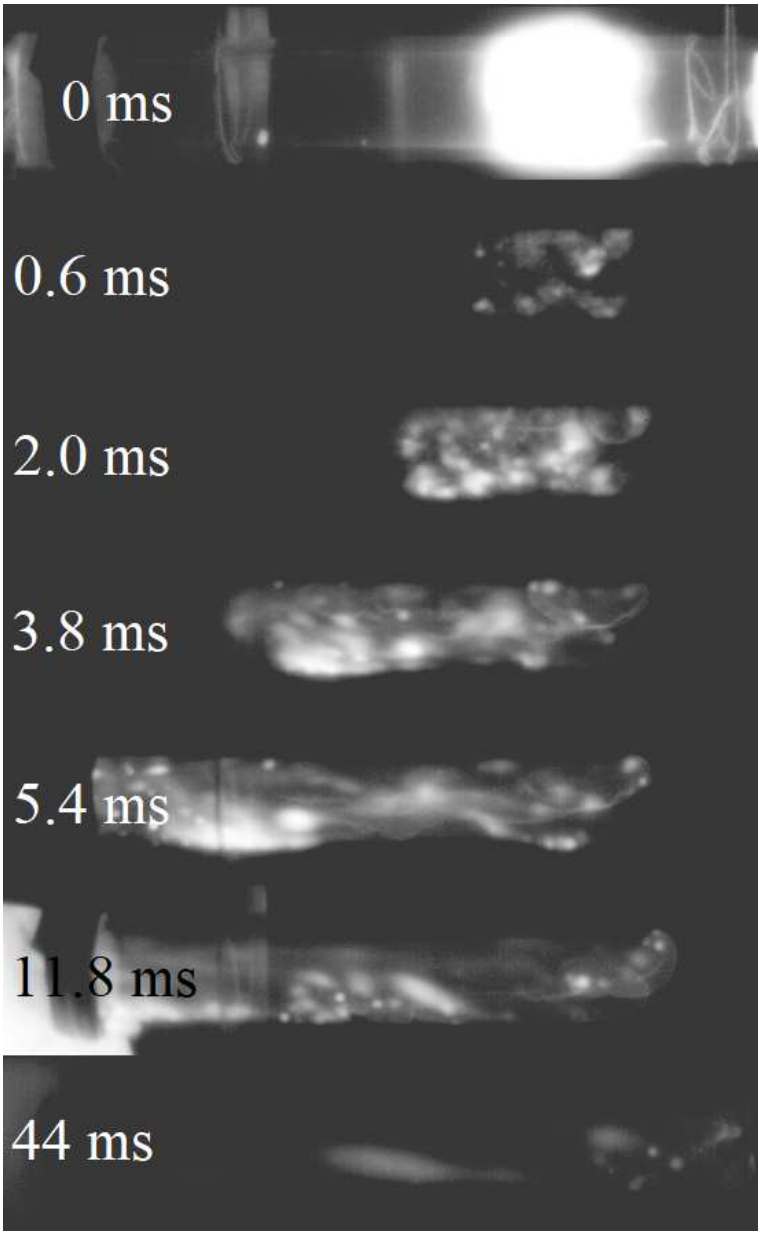

Figure 3: A typical sequence illustrating development of the combustion. The length of the area span by the net of streamers is 55 mm. A "piston" of hot gas expands towards the open (left) end of the tube at approximately 50 m/s while the flame slowly, at the level of 1 m/s propagates in the stationary gas towards the closed (right) end of the tube.

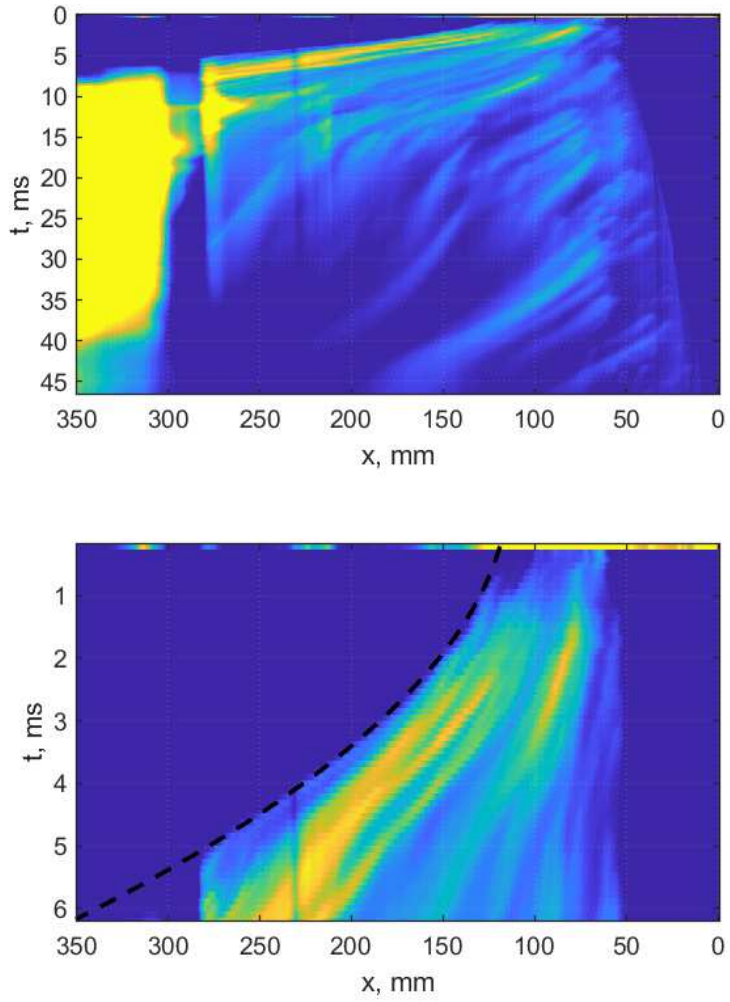

Figure 4: A typical spatio-temporal diagram used for visualisation of the evolution of the area occupied by combustion products and hence measurement of propagation speed of the flame. The whole diagram is shown at the top and the zoomed-in interval of the first 6 millisecond after the discharge is shown at the bottom. Bright areas correspond to areas spanned by flame, as can be compared with the image sequence in Fig. 3. The slope of the flame-occupied area corresponds to the propagation speed. Oscillations at the tube closed (right) end visible up to 10 ms after the discharge correspond to pressure oscillations. The dashed line corresponds to the model (9)

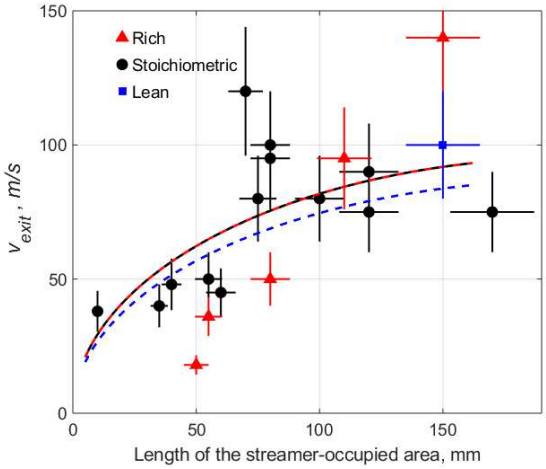

Figure 5: Dependence of the speed of propagation of the visible combustion front when it exits the tube on the length of the area occupied by the streamer discharge initiated on the internal surface of the tube. Lines show the modelled velocity (8) at the tube exit for stoichiometric/rich mixtures (solid line) and lean mixture (dashed line).

increase the apparent ignition volume. Then, turbulent flow occurring in the tube may speed up the flame propagation rate. A simple model presented below suggests the first factor, the large area of the flame front, quantitatively explains the observed axial flame propagation.

Consider evolution of combustion products formed in the volume span by the streamer with the network of streamers occupying L_{ign} part of the tube of $L_{tube} = 300$ mm length and $r_{tube} = 15$ mm inner radius. Back of the envelope estimates of the pressure needed to axially accelerate the gas column combined with visual assessment of the flame boundary oscillations at the closed end of the tube (right boundary of the flame in Fig.4) suggest that the deviation of the pressure inside the tube from the atmospheric does not exceed 20%. Therefore, we further assume the pressure of the unburned mixture is $P_0 = 10^5$ Pa.

Recalling that the mass fraction of propane in stoichiometric mixture is $\Phi_{C_3H_8} = 0.064$ and the heat capacity of Propane is $\lambda = 46$ MJ/kg, we get the energy released per unit length of the streamer channel due to the instant

combustion as

$$\varepsilon_{str} \sim \pi r_{str}^2 \cdot \lambda \rho_0 \Phi_{C_3H_8} \sim 1.4 \text{ J/m} \tag{1}$$

Here, the mixture density is taken at atmospheric pressure and the room temperature as $\rho_0 = 1.2$ kg/m^3 and the radius of the streamer channel from [26] as $r_{str} \sim 0.35$ mm. Now, we have a configuration where hot combustion products form a network of thin cylindrical channels. As channel radius r_{str} is much less than length of network segments (Fig. 3), for the sake of simplicity they will be treated as infinitely long and axisymmetric. We refer to the work [31] on cylindrical shocks to calculate, at 1.2 J/m energy input, the characteristic radius in the system as

$$R^* = \sqrt{\varepsilon_0/\gamma P_0} \approx 3\text{mm} \tag{2}$$

and hence the characteristic time defined by the speed of sound in the unperturbed gas at 9 μs. Using density plots from numerical results reported in [31] we conclude that, within microseconds, i.e. instantly in our observation timescale, the channels of hot combustion products expand to $r_0 \sim 0.3R^* \sim 0.9$mm. From here, combustion front propagates with the laminar velocity v_0 outwards at the surface of expanded streamer channels. The volume of unburned gas consumed by flames per unit time is

$$\frac{dV_{unburned}}{dt} = \ell_{str} \cdot 2\pi r \cdot v_0 \tag{3}$$

where ℓ_{str} is the total length of burned out channels, r is their radius, and $v_0 = 0.4$ m/s is the laminar flame propagation velocity. Evaluating, from Fig. 2, the typical distance between streamers as $h \sim 4$ mm, we estimate the total length of the streamer channels as

$$\ell_{str} \sim 2\pi r_{tube} \cdot L_{ign}/h \tag{4}$$

which, in the strongest discharges we use, exceeded 3 metres. Assuming that combustion products expand adiabatically (which is not the case but suitable

for the order of magnitude estimate), the rate of expansion of the gas contained within the tube is

$$\frac{dV}{dt} = \frac{dV_{unburned}}{dt} \cdot \left(\frac{P_1}{P_0}\right)^{1/\gamma} = \frac{dV_{unburned}}{dt} \cdot \beta_{exp} \tag{5}$$

Here, we have introduced the gas expansion ratio β_{exp} which depends on the ratio of pressures after and before instantaneous combustion P_1/P_0 which is essentially ratio of temperatures of combustion products and the initial gas mixture:

$$\beta_{exp} = \left(\frac{P_1}{P_0}\right)^{1/\gamma} = \left(\frac{T_1}{T_0}\right)^{1/\gamma} = \left(1 + \frac{\Phi_{C_3H_8} \cdot \lambda}{c_V \cdot T_0}\right)^{1/\gamma} \approx 6.8. \tag{6}$$

For simplicity, we have assumed the adiabatic constant and the heat capacity of the resulting mixture being equal to that of air $\gamma = 7/5$, $c_V \sim 718$ J/kg. As the speed of flame propagation in stationary mixture is v_0, the radius of burned out channels evolves as

$$r = r_0 + \beta_{exp} \cdot v_0 t \tag{7}$$

The apparent speed of combustion region expansion along the tube is its volume expansion rate divided by the tube cross-section, hence we get

$$U_{apparent} = \frac{2\pi \left(r_0 + \beta_{exp} \cdot v_0 t\right) \ell_{str}}{\pi r_{tube}^2} \beta_{exp} \cdot v_0 \tag{8}$$

Integrating 8 in time and using (4), we get, for the axial coordinate of the visible combustion front,

$$X_{apparent} = L_0 + \frac{4\pi v_0}{h r_{tube}} \left(r_0 t + \frac{1}{2} v_0 \beta_{exp} t^2\right) \beta_{exp} \cdot L_{ign} \tag{9}$$

The modelled position of the apparent flame front is shown in Fig. 4 by a dashed line. To make the curve fit the observed front trajectory, the coefficient β_{exp} in (6) has been set to 3.1 (as in equation (6) divided by 2.2) which seems
145 a reasonable adjustment provided crudeness of the model.

To test the model against other measurements, the apparent flame speed at the exit of the tube was measured and compared to that predicted by (8). Solving the quadratic equation (9) with respect to t, we find the time instant

when flames leave the tube. Substituting that to (8), we find the apparent flame speed at the tube exit which are plotted in Fig. 5 together with the measured flame exit velocities. When calculating the curve, same expansion ratio β_{exp} has been used as that to plot the curve in Fig. 4(b). This seemingly random adjustment of (6) may reflect the heat conduction loss from the laminar flame front leading to weaker-than-adiabatic expansion of combustion products.

A factor which has not been accounted for yet is the autoignition. The temperature of combustion products immediately after the streamer ignition is $T_1 \sim 300$ K $+ \Phi_{C_3H_8}\lambda/c_V \sim 4400$ K, hence temperature at the location of the igniting streamer is well in excess of a typical autoignition temperatures from 1200K to 1800K mentioned in [32], where the autoignition delays from 10 μs to 500 μs have been reported. The study [33] suggests similar autoignition delays in a range of pressures. The above timescales are within the first two frames in Fig. 4 and therefore gas mixture autoignition may take place unnoticed in our experiments. From energy balance, the temperature of 1200K can be reached in the volume spanning as much as four cross-sections or two diameters of the streamer. While potentially doubling the initial radius of the burning filaments r_0 in (8) this will not significantly influence the flame propagation speed achieved at the tube exit. Another possible source of ignition is the over-pressurisation by the shock wave initiated by the streamer discharge. We evaluate the autoignition-prone volume of the gas-fuel mixture using results on cylindrical shocks reported in [31]. With the characteristic radius $R^* = 3$mm from (2) and the characteristic time of 9 μs, simulations suggest that, in our parameter range, significant over-pressurization only occurs at timescales of single microseconds which is too short for the autoignition to take place.

Another flame accelerating mechanism is the flow turbulence. Indeed, studies [34, 35] report up to 10-fold increase in the flame propagation speed due to turbulence when the turbulence intensity is high enough i.e. when the velocity of turbulent fluctuations reaches 10 or so laminar flame velocities which may be the case in our experiments. Meanwhile, analysis of high speed videos suggests that turbulence does not form in the tube with the tube-diameter-size flow

structures persist throughout the gas expansion as clearly seen seen in frames 0.8, 1.4, and 2.0 ms in Fig. 3.

The volumetric ignition by the network of streamer channels comes at a cost. The energy absorbed by the streamer from the microwave radiation can be approximately evaluated from the magnitude of Poynting vector, the energy density $\langle S \rangle$, in the incident microwave radiation and the absorbing cross-section taken as the tube cross-section.

$$E_{streamer} = \langle S \rangle A_{tube} \cdot \Delta t = \frac{E_{max}^2}{2\eta_0} \cdot \pi r_{tube}^2 \cdot \Delta t \tag{10}$$

where $\eta_0 = 337\ \Omega$ is the impedance of vacuum, $E_{max} \approx 2 \cdot 10^5$ V/m is the amplitude of electric field near the focus and $\Delta t \approx 40\mu$s is duration of the microwave pulse. The strongest discharges we used (right end of the curve in Fig. 5) absorb the energy at the level of 2 J while the typical energy discharged by a car spark plug is an order of magnitude less at 0.1 J. The energy absorbed by the streamer network $E_{streamer}$ is essentially independent of its length, therefore for practical applications the streamer discharge length should be maximised, for example, by using a parallel, not focussed, microwave beam or by placing the combustion chamber into a waveguide.

We note that energy released by the streamer per unit length is of the same order but a few times less than the chemical energy (1) released by the gas it spans hence does not significantly affect our model (8).

5. Conclusion

When the energy density necessary for ignition of the air-fuel mixture is reached, the surface area of ignition region becomes a key parameter to increase the speed of combustion. We have investigated ignition by a microwave streamer discharge representing a network of plasma filaments that initiate ignition. Unlike in laser ignition, combustion is being seeded along a network of lines, not at points, which changes the problem symmetry from spherical to cylindrical. A high amount of energy is being released by the nearly instantaneous combustion

of large amount of gas mixture along a randomly-shaped network of streamer channels. As a result, a large area flame front forms at the channels' surface before any flame-accelerating turbulence has a chance to appear. The effect of ignition volume on the propagation of flame in air-propane mixture has been investigated experimentally in axisymmetric configuration and compared to a simple mathematical model.

A stable ignition of the premixed air-propane mixture with the subcritical streamer discharge initiated on the internal surface of a cylindrical acrylic tube has been achieved at 20°C and atmospheric pressure. Ignition of the air-propane mixture by a subcritical streamer discharge yields more than a 200-fold, from 0.4 m/s to above 100 m/s, increase in the apparent speed of flame propagation compared to the laminar flame propagation.

The rapid combustion achieved by ignition by the streamer discharges can be exploited in practical combustion devices. The new ignition systems can be implemented in internal combustion engines and premixed gas turbines. The microwave streamer ignition can be considered for the application in internal combustion engines to replace the conventional spark ignition. Creating preconditions for deflagration to detonation transition, the streamer ignition can also be applied to pulsed detonation engines currently being evaluated for high-speed propulsion systems.

Acknowledgements

This work was financially supported by the Ministry of Education and Science of Russian Federation (agreement No 14.577.21.0277, unique identifier of applied scientific research RFMEFI57717X0277).

References

References

[1] Y. Ju, K. Maruta, Microscale combustion: technology development and fundamental research, Progress in Energy and Combustion Science 37 (6)

(2011) 669–715. doi:10.1016/j.pecs.2011.03.001.

[2] B. Wolk, A. DeFilippo, J.-Y. Chen, R. Dibble, A. Nishiyama, Y. Ikeda, Enhancement of flame development by microwave-assisted spark ignition in constant volume combustion, Combustion and Flame 160 (7) (2013) 1225–1234. doi:10.1016/j.combustflame.2013.02.004.

[3] T. Phuoc, Single-point versus multi-point laser ignition: experimental measurements of combustion times and pressures, Combustion and Flame 122 (4) (2000) 508–510. doi:10.1016/S0010-2180(00)00137-1.

[4] A. Hossain, N. Oshima, Y. Nakamura, M. Oshima, Numerical investigation of the effect of ignition area on the subsequent flame propagation behavior, Journal of Thermal Science and Technology 4 (2) (2009) 214–225. doi:10.1299/jtst.4.214.

[5] I. Matveev, S. Matveeva, S. Serbin, Design and preliminary result of the plasma assisted tornado combustor, Proc. 43rd AIAA/ASME/SAE/ASEE Joint Propulsion Conference and Exhibit (2007) 2007–5628doi:10.2514/6.2007-5628.

[6] I. Matveev, S. Serbin, Investigation of a reverse-vortex plasma assisted combustion system, Proceedings of the ASME Heat Transfer Summer Conference, Puerto Rico, USA HT2012-58037 (2012) 133–140. doi:10.1115/HT2012-58037.

[7] M. Nettleton, Gaseous detonations: their nature, effects and control, Springer Science and Business Media, 2012.

[8] W. Wu, C. Fuh, C. Wang, Comparative study on microwave plasma-assisted combustion of premixed and nonpremixed methane/air mixtures, Combustion Science and Technology 187 (2015) 999–1020. doi:10.1080/00102202.2014.993032.

[9] A. Starikovskiy, N. Aleksandrov, A. Rakitin, Plasma-assisted ignition and deflagration-to-detonation transition, Philos Trans A Math Phys Eng Sci 370 (2012) 740–773. doi:10.1098/rsta.2011.0344.

[10] A. Napartovich, I. Kochetov, S. Leonov, Calculation of the dynamics of ignition of an air hydrogen mixture by nonequilibrium discharge in a high-velocity flow, High Temperature 43 (5) (2005) 673–679. doi:10.1007/s10740-005-0110-8.

[11] A. Starik, V. Kozlov, N. Titova, On the influence of singlet oxygen molecules on the speed of flame propagation in methane-air mixture., Combustion and Flame 157 (2) (2010) 313–327. doi:10.1016/j.combustflame.2009.11.008.

[12] S. Starikovskaia, Plasma assisted ignition and combustion, Journal of Physics D: Applied Physics 39 (16) (2006) 265–299. doi:10.1088/0022-3727/39/16/R01.

[13] N. Popov, The effect of nonequilibrium excitation on the ignition of hydrogen–oxygen mixtures, High Temperature 45 (2) (2007) 261–279. doi:10.1134/S0018151X07020174.

[14] S. Leonov, D. Yarantsev, Plasma-induced ignition and plasma-assisted combustion in high-speed flow, Plasma Sources Science and Technology 16 (1) (2007) 132–139. doi:10.1088/0963-0252/16/1/018.

[15] G. Correale, A. Rakitin, A. Nikipelov, S. Pancheshnyi, I. Popov, A. Starikovskiy, T. Shiraishi, T. Urushihara, M. Boot, Non-equilibrium plasma ignition for internal combustion engines, SAE Technical Paper (2011) 2011–24–0090doi:10.4271/2011-24-0090.

[16] J. Lefkowitz, P. Guo, T. Ombrello, S.-H. Won, C. Stevens, J. Hoke, F. Schauer, Y. Ju, Schlieren imaging and pulsed detonation engine testing of ignition by a nanosecond repetitively pulsed discharge, Combustion and

Flame 162 (6) (2015) 2496–2507. doi:10.1016/j.combustflame.2015.02.019.

[17] M.Uddi, H. Guo, W. Sun, Y. Ju, Studies of c_2h_6/air and c_3h_8/air plasma assisted combustion kinetics in a nanosecond discharge, Proc. 49th AIAA Aerospace Sciences Meeting Including the New Horizons Forum and Aerospace Exposition (2011) AIAA–2011–970.

[18] C. Stevens, F. Pertl, J. Hoke, F. Schauer, J. Smith, Comparative testing of a novel microwave ignition source, the quarter wave coaxial cavity igniter, Proc. of the Institution of Mechanical Engineers D: Journal of Automobile Engineering 225 (12) (2011) 1633–1640. doi:10.1177/0954407011411389.

[19] C. Fuh, W. Wu, C. Wang, Microwave plasma-assisted ignition and flame holding in premixed ethylene/air mixtures, Journal of Physics D: Applied Physics 49 (2016) 285202. doi:10.1088/0022-3727/49/28/285202.

[20] Y. Ju, F. Dryer, University Capstone Project: Enhanced Initiation Techniques for Thermochemical Energy Conversion, Princeton University, 2013.

[21] R. Khoronzhuk, A. Karpenko, V. Lashkov, D. Potapeko, I. Mashek, Microwave discharge initiated by double laser spark in a supersonic airflow., Journal of Plasma Physics 81 (2015) 905810307. doi:10.1017/S0022377814001299.

[22] J.-L. Beduneau, B. Kim, L. Zimmer, Y. Ikeda, Measurements of minimum ignition energy in premixed laminar methane/air flow by using laser induced spark, Combustion and Flame 132 (4) (2003) 653–665. doi:10.1016/S0010-2180(02)00536-9.

[23] T. Shiraishi, T. Urushihara, M. Gundersen, A trial of ignition innovation of gasoline engine by nanosecond pulsed low temperature plasma ignition, Journal of Physics D: Applied Physics 42 (13) (2009) 135208. doi:10.1088/0022-3727/42/13/135208.

[24] I.Esakov, L. Grachev, K. Khodataev, D. V. Wie, The linear electromagnetic vibrator as the initiator of electric breakdown of air in deeply subcritical field of quasioptical microwave beam, 49th AIAA Aerospace Sciences Meeting Including the New Horizons Forum and Aerospace Exposition (2011) AIAA–2011–1151doi:10.2514/6.2011-1151.

[25] L. Grachev, I. Esakov, K. Khodataev, Features of the development of pulsed microwave discharges in various gases in a quasioptical beam, Technical Physics 43 (4) (1998) 378–381. doi:10.1134/1.1258990.

[26] K. Aleksandrov, L. Grachev, I. Esakov, K. Khodataev, Surface streamer microwave discharge, Technical Physics 47 (7) (2002) 851–855. doi:10.1134/1.1495046.

[27] K. Aleksandrov, L. Grachev, I. Esakov, V. Fedorov, K. Khodataev, Domains of existence of various types of microwave discharge in quasi-optical electromagnetic beams, Technical Physics 51 (11) (2006) 1448–1456. doi:10.1134/S1063784206110090.

[28] A. MacDonald, Microwave breakdown in gases, New York, London, Sydney: John Wiley & Sons, 1966.

[29] T. Langer, D. Markus, F. Lienesch, U. Maas, Ignition of hydrogen/air mixtures by streamer discharges, Proceedings of the 4th European Combustion Meeting, Vienna, Austria (2009) 1–6.

[30] M. S. Ebaid, K. J. Al-Khishali, Measurements of the laminar burning velocity for propane: Air mixtures, Advances in Mechanical Engineering 8 (6) (2016) 1–17. doi:10.1177/1687814016648826.

[31] M. N. Plooster, Shock waves from line sources. numerical solutions and experimental measurements, Physics of Fluids 13 (11) (1970) 2665–2675. doi:10.1063/1.1692848.

[32] D. C. Horning, D. F. Davidson, R. K. Hanson, Study of the high-temperature autoignition of n-alkane/o/ar mixtures, Journal of Propulsion and Power 18 (2) (2002) 363–371. doi:10.2514/2.5942.

[33] R. Bounaceur, P.-A. Glaude, B. Sirjean, R. Fournet, P. Montagne, M. Vierling, M. Molière, Prediction of auto-ignition temperatures and delays for gas turbine applications, J. Eng. Gas Turbines Power 138 (2) (2016) 021505. doi:10.1115/1.4031264.

[34] S. S. Shy, W. J. Lin, J. C. Wei, An experimental correlation of turbulent burning velocities for premixed turbulent methane-air combustion, Proc. R. Soc. Lond. A 456 (2000) 1997–2019. doi:10.1098/rspa.2000.0599.

[35] E. M. Burke, F. Güthe, R. F. D. Monaghan, A comparison of turbulent flame speed correlations for hydrocarbon fuels at elevated pressures, ASME. Turbo Expo: Power for Land, Sea, and Air 4B: Combustion, Fuels and Emissions (2016) V04BT04A043. doi:10.1115/GT2016-57804.